Wetting prevention in membrane distillation through superhydrophobicity and recharging an air layer on the membrane surface

Wetting prevention in membrane distillation through superhydrophobicity and recharging an air layer on the membrane surface

Mohammad Rezaei [a,], David M. Warsinger [b], John H. Lienhard V [b], Wolfgang M. Samhaber [a]*

[a] Institute of Process Engineering, Johannes Kepler University Linz, Altenberger Strasse 69, 4040 Linz, Austria

[b] Rohsenow Kendall Heat Transfer Laboratory, Department of Mechanical Engineering Massachusetts Institute of Technology, 77 Massachusetts Avenue, Cambridge MA 02139-4307 USA

*Corresponding Author: Tel: +4373224689747, E-mail: mohammad.rezaei@jku.at

Cite this article as:
Mohammad Rezaei, David M. Warsinger, John H. Lienhard V, and Wolfgang M. Samhaber, Wetting prevention in membrane distillation through superhydrophobicity and recharging an air layer on the membrane surface, Journal of Membrane Science, 530 (2017): 42-52.
http://dx.doi.org/10.1016/j.memsci.2017.02.013

Abstract

Although membrane distillation offers distinctive benefits in some certain areas, i.e., RO concentrate treatment, concentrating solutions in the food industry and solar heat utilization, the occurrence of wetting of the hydrophobic membrane hinders its potential industrial applications. Therefore, wetting prevention is a vital criterion for the treatment of solutions with lower surface tension than water. The present work examines the effect of recharging air bubbles on the membrane surface for the wetting incidence when a surfactant (sodium dodecyl sulfate, SDS) exists in a highly concentrated NaCl aqueous solution. This study shows that the presence of the air bubbles on the surface of the superhydrophobic membrane in a direct contact membrane distillation setup inhibited the occurrence of wetting (~100% salt rejection) even for high concentrations of the surface-active species (up to 0.8 mM SDS) in the feed solution while no undesirable influence on the permeate flux was observed. Introducing air into the feed side of the membrane displaces the liquid which partly tends to penetrate the macroporous structure with air bubbles and therefore increases the liquid entry pressure, and in addition, the simultaneous use of a superhydrophobic membrane enhances the solution contact angle.

Keywords: Membrane distillation; Wetting phenomenon; Air recharging; Superhydrophobic membrane

1. Introduction

Membrane distillation is a thermally driven membrane process that utilizes a porous hydrophobic membrane for separating components in a liquid mixture based on their volatility. The driving force in MD relies on the difference in vapor pressure of the volatile component that is induced by a transmembrane temperature difference. Mass transfer through the membrane pores only takes place in the vapor phase, from a hot feed solution to a cooled permeate condensate [1]. Therefore, the liquid feed must be prevented from penetrating partially or entirely through the dry pores of the membrane. When pore wetting occurs, it will at the least impair product quality or at most will incapacitate the process. A primary advantage of MD is the high salt rejection (99.9%+), and pore wetting can cause rejection to fall below 85%, ruining the process [2].

Recently, a new approach has been created to mitigate membrane wetting, by continually adding in the air to the feed side of the process, effectively reducing the fraction of the membrane area in contact with the liquid, and depinning liquid from inside the membrane pores. Some authors have also concluded that existence of the air gap could provide an opportunity to increase mass flux [3]. When measuring foulant mass adhered, this new method has been shown to be very effective in mitigating biofouling [4], and also effective in reducing inorganic scaling and particulate fouling [5]. However, those studies used membranes in stirred-cells and not full MD systems. Prior to this work, the impact of air recharging has not been studied in full MD systems, has not examined spacers for improving air trapping, and has not been tested for wetting prevention or the impact of permeate flux.

Hydrophobic MD membranes are always associated with the pore wetting problem. Wetting restricts MD for some practices such as desalination, removal of trace volatile organic compounds

from wastewater and concentration of ionic, colloids or other non-volatile aqueous solutions [6,7], and other solutions with high fouling propensity. Similar to using thinner membranes, significant partial wetting into the membrane may reduce its effective thermal conductivity and thus decrease the MD thermal efficiency, resulting in permeate flux reduction [8]. But, when complete pore wetting occurs due to water bridging, the permeate flux of membrane increases with time.

Membrane wettability can be characterized by Liquid Entry Pressure (LEP, occasionally incorrectly named "wetting pressure"). The "Round Table" at the "Workshop on Membrane Distillation" in Rome on May 5, 1986, defined LEP as the pressure that must be applied to pure water before it enters into a non-wetted membrane [9]. LEP can be calculated by the Young-Laplace equation

$$LEP = \frac{4B\ \gamma_l\ cos\theta}{d_{max}} \qquad (1)$$

where LEP is the entry pressure difference, γ_l is the surface tension of the solution, θ is the angle of contact between the solution and the membrane surface, d_{max} is the largest pore size, and B is a geometric factor influenced by the pore structure with a value equal to one for cylindrical pores [10].

When organic compounds or surfactants exist in the feed solution, LEP decreases and the membrane pores may wet. LEP depends on the pore diameter, the geometric structure of the pores, surface tension of the liquid with vapor, and the contact angle between the membrane surface, the liquid, and vapor phases. Membranes with small pore size, narrow pore size distribution, ideal cylindrical pore geometry, low surface energy, high contact angle, and high roughness typically show higher LEP. However, LEP cannot properly describe the happening of membrane wetting. For instance, some membranes have been reported not to wet at all despite their LEP value of zero

(CA=90°), which indicates an immediate wetting even at a transmembrane pressure of only 0.1 kPa. In contrast, some other membranes with LEP of 42 kPa and 32 kPa experienced wetting [11]. Those authors concluded that the occurrence of wetting could not be justified by the LEP value, but relates tightly with the existence of micro-scale defects. Still, membranes with higher LEP have shown corresponding higher fouling resistance and significantly reduced wetting.

Although wetting prevention in MD is the main process requirement, it has not been comprehensively studied and relatively few investigations have attempted to solve the wetting problems in MD membranes [12–20]. Some authors have investigated the improvement of hydrophobic properties of membranes employing novel materials or applying surface modification through manipulating surface chemistry and surface geometry by nanoparticle coating and surface fluorination [21–27]. However, these membranes are still susceptible to pore wetting when treating feed solutions containing a high concentration of surface-active species. Other authors have studied the effect of operating parameters on the wetting process and suggested that increasing feed temperature can slow the wetting process by reducing the absolute pressure in the feed side, and consequently the driving force for the Poiseuille flow and increase the distillate diluting effect [28]. However, this is mentioned to be helpful after the occurrence of membrane partial pore wetting. Some authors reported that delaying membrane wetting by using membrane distillation bioreactors allows the system to keep a high total organic removal efficiency of 99.9% for an extended operation time (in contrast to standalone MD systems). Nevertheless, their system still needed membrane cleaning and drying after wetting occurrence [29]. Several authors have placed spacers in MD modules and have carried out experimental and theoretical investigations on the subject [30–34]. In their results, they published notable enhancement on heat and mass transfer and consequently the mass flux in spacer filled modules and provided suggestions on optimal

spacer geometry, voidage, and hydrodynamic angle [35]. Although these approaches are meaningful, robust solutions are needed to prevent wetting permanently.

The main objective of this paper is to show the effect of air recharging near the surface of the membrane on the wetting phenomenon, using hydrophobic polypropylene (PP) and superhydrophobic polytetrafluoroethylene/polyethersulfone (PTFE/PES) membranes. In such a system, numerous direct contact membrane distillation (DCMD) experiments were carried out to study also the influence of mesh spacer existence in the feed and permeate side of the membrane on wetting control. For reaching wetting condition, SDS was added stepwise to a high concentration of NaCl aqueous solution to decrease steadily the surface tension of the feed.

2. Theoretical section

The impact of increasing the air fraction via air recharging can be examined using Cassie's law (equation 2), which gives an effective contact angle for a surface containing multiple materials (materials 1 and 2) [36].

$$\cos(\theta_c) = f_1 \cos(\theta_1) + f_2 \cos(\theta_2) \qquad (2)$$

Where θ_c is the effective contact angle and f_1 and f_2 are the area fractions of materials 1 and 2, and sum to 1. Here θ_1 and θ_2 are the contact angles for the materials. Notably, the contact angle of air is 180°. Equations (1) and (2) can be combined to examine the impact of air recharging on LEP (Fig. 1).

As seen in Fig. 1, the presence of air can dramatically improve the LEP of the membrane, especially for less hydrophobic materials. Diminishing returns are reached for very high contact angles (>150°). Notably, the contact angles here are for the surface material itself, which is typically lower than that measured on membranes, since the membrane roughness already traps

some air in those measurements. Therefore, the benefit of increasing the air fraction is still expected to be large for very hydrophobic membranes. For example, the contact angle of the PTFE/PES membranes used was 153°, while PTFE itself has a contact angle of about 109°.

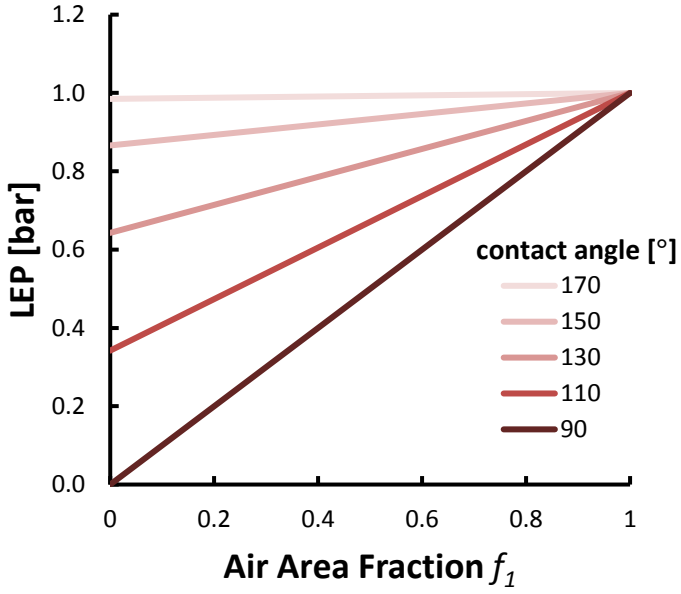

Fig. 1. LEP versus the air area fraction f_1 for membrane materials of different contact angles. Representative values are chosen for B (1) and d_{max}(4 μm) for the Young-Laplace Equation.

3. Experimental section

3.1 Materials

Flat sheet Accurel® hydrophobic polypropylene and Tetratex® superhydrophobic polytetrafluoroethylene membranes from Enka and Donaldson are used. Table 1 summarizes the properties of the PP and PTFE membranes used in this study.

The superhydrophobic membrane chosen has been proven to be an effective MD membrane in the past, and was created using a stretching technique, and bonded to a Reemay 2275 polyester nonwoven support layer [37]. Sodium dodecyl sulfate (99%) as a wetting agent and sodium

chloride (NaCl) are obtained from Sigma–Aldrich. SDS was chosen as wetting liquid due to the lower surface tension than water, which makes it more penetrative in the pores of the membrane.

Table 1. Properties of polymeric membranes.

Membrane trade name	Polymer	Thickness (μm)	Nominal pore size (μm)	IPA bubble point (kPa)	Air flowrate (l/min/cm^2 @ 0.7 bar)	Contact angle
Accurel 2E-PP	PP	177	0.2	114.5	1.3	113°
Tetratex 6532	PTFE/ PES	130	0.1	200	3	153°

3.2 Membrane cell

A plate and frame membrane cell was used to conduct the DCMD experiments. It consists of two sandwiched polyvinylidene fluoride (PVDF) disk cells with the membrane in between providing an effective contact area of 0.01 m^2. The cell has open flow channels in both feed and permeate sides, including mesh spacer for supporting membrane stability and air distributors for dispensing air bubbles.

Spacer channels are used to enhance the hydrodynamic conditions at the membrane surface [38]. For some experiments, a mesh spacer on the feed side of the membrane cell was placed to increase trapping the air bubbles on the membrane surface. Table 2 summarizes the specifications of flow channels and the mesh spacers. Further care needs to be considered regarding the location of the spacer, as the applied pressure on the particular places of the membrane by the spacer may intensify the pore wetting incident [39]. Before each experiment, the cell was inspected for any water leakage.

3.3 Methods

The experiments started with deionized water as feed and permeate. After 30 minutes, NaCl was added to the feed side to make a solution of 1.0 M NaCl for examining the pore wetting and flux variations in highly concentrated saline water. In order to decrease progressively the surface tension of the feed solution, 0.1 mM SDS in the intervals of 30 minutes was sequentially added to the feed solution [40]. After wetting was noticed, experiments were proceeded to study the wetting phenomenon for the whole area of the membrane for a longer time. The experiments were stopped when a rapid reduction of the salt rejection factor or a sharp rise in the permeate flux obtained. Based on the salt rejection, the concentration of SDS in feed solutions for different experiments was varied between 0.3 to 0.8 mM.

Table 2. Specifications of flow channels and mesh spacers.

Channel or Spacer Property	Value
Mesh spacer material	PP
Mesh spacer void fraction	0.708
Number of flow channel	4
Hydraulic diameter of flow channel (m)	0.202
Length of flow channel (m)	0.1
Width of flow channel (m)	0.23
Height of flow channel (m)	0.18

The performance of the membranes and air changing in a DCMD setup were measured (Fig. 2). The membrane cell was sloped to retain the flow of air bubbles on the surface of the membrane, where the feed solution circulated from the bottom of the cell. The air was filtered through a 0.2 μm hydrophobic Sartofluor® polytetrafluoroethylene membrane prior to the recharging to remove the air particulates and microorganisms which may cause bio-fouling and consequently lead to

membrane wetting. Permeate and feed inlet temperatures were set to 20 °C and 60 °C. The mean bulk feed and bulk permeate temperature difference was kept to 35 °C to obtain a high driving force. In all the experiments, a higher feed cross flow rate than permeate was applied to facilitate the detection of membrane wetting. This is because it causes a higher hydraulic pressure for feed side, and when pore wetting occurs, it prevents the reverse flow of the permeate to the feed side. This will lead to membrane pore wetting identification by increasing the permeate electrical conductivity due to the flow of the liquid feed solution to the permeate side through wetted membrane pores. To prevent instant membrane wetting, the transmembrane hydrostatic needs to be lower than the LEP [41]. Therefore, the pressure gradient through the membrane (0.1 bar) was controlled continuously by monitoring two manometers placed at the feed and permeate sides of the membrane module. The conductivity of the permeate solution was measured continuously to identify the incident of membrane wetting. Table 3 shows the range of the operating conditions for different experimental setups.

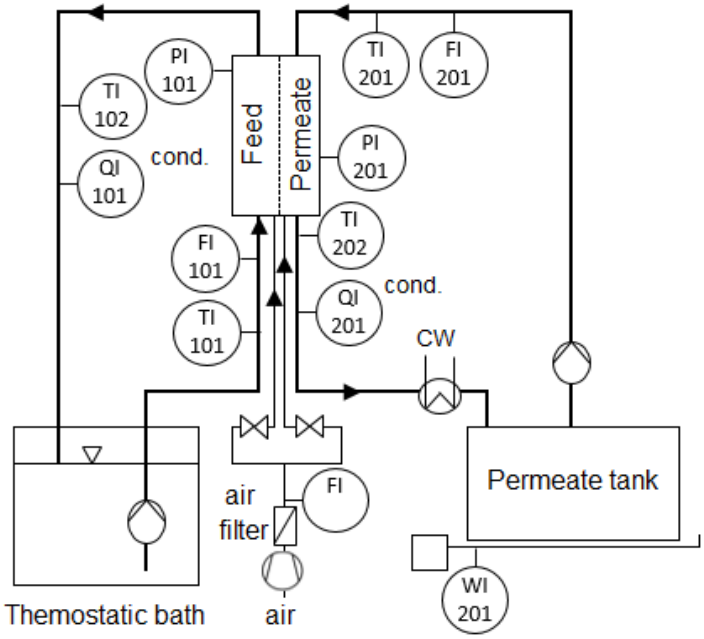

Fig. 2. Schematic diagram of the lab-scale DCMD setup. TI, FI, PI, QI and WI are temperature, flow, pressure, quality (i.e., electrical conductivity) and weight indicators, respectively.

Table 3. Range of operating conditions

Feed inlet temp. (°C)	Feed outlet temp. (°C)	Permeate inlet temp. (°C)	Permeate outlet temp. (°C)	Transmembrane pressure difference (bar)	Liquid feed inlet flow rate (L/h)	Permeate inlet flow rate (L/h)	Air flow rate (L/h)
59.5-61.5	57.5-59.5	17.3-19.5	22.5-25.4	Max.~0.1	30	12	100

In order to investigate the effect of the air recharging and presence of the mesh spacer on membrane pore wetting, several experimental configurations were defined. Two default configurations were defined for the systems with hydrophobic or superhydrophobic membranes and without air bubbles and mesh spacers. Table 4 shows the different configurations studied in this work. The air was introduced by continuously purging air flow through the air distributor placed at the bottom of the cell in the feed or permeate sides of the membrane. To eliminate measurement error, each set of experiments was carried out three times and the mean of these measured values and the maximum positive and negative difference from the mean were calculated and included as uncertainty bars in the presented data.

Table 4. Experimental configurations. "+" and "-" correspond to the existence and non-existence of that parameter, respectively.

Experiment setup	Membrane	Feed side		Permeate side	
		Air recharging	Spacer	Air recharging	Spacer
E1 (Default 1)	PP	-	-	-	-
E2	PP	-	+	+	+
E3	PP	+	-	-	+
E4 (Default 2)	PTFE	-	-	-	-
E5	PP	+	+	-	+
E6	PTFE	+	+	-	+

To better estimate the feed circulation flux, the two-phase flow Reynolds number is calculated based on the method from H. Groothuis et al. [42]:

$$Re_{tp} = Re_l + Re_g = \frac{dU_l\rho_l}{\mu_l} + \frac{dU_g\rho_g}{\mu_g} \qquad (2)$$

where Re_{tp} is air/liquid two-phase flow Reynolds number, Re_l and Re_g are liquid and air phase Reynolds numbers; $Re_l=dU_l\rho_l/\mu_l$, $Reg=dU_g\rho_g/\mu_g$, d is the hydraulic diameter (m), U_l and U_g are the superficial velocities of liquid and air (m/s), μ_l and μ_g are the dynamic viscosities of liquid and air (kg/(m·s)), ρ_l and ρ_g are the densities of the liquid and air (kg/m3). The Reynolds number for the feed solutions with air recharging in the setups E3, E5 and E6 was 168 and Reynolds number of permeate with the air recharging for the setup E2 was 85.

The effectiveness of air recharging and mesh spacer existence on membrane pore wetting was determined by measuring the salt rejection and the permeate flux in comparison with the default systems. Salt rejection, water flux, wetting factor, concentration factor and water recovery were calculated using following equations:

$$R = \left(1 - \frac{C_{b,p}}{C_{b,f}}\right)100 \qquad (3)$$

$$\mathrm{J} = \frac{\Delta m_p}{A\,\Delta t} \qquad (4)$$

$$WF = \frac{J_t - J_i}{J_i} \qquad (5)$$

$$CF = \frac{M_{Fi}}{M_{Fi} - M_{Pj}} \qquad (6)$$

$$WR = 100\frac{M_{Pj}}{M_{Fi}} = 100\left(1 - \frac{1}{CF}\right) \qquad (7)$$

where R is the salt rejection, $C_{b,p}$ and $C_{b,f}$ are the salt concentration in permeate and feed solutions, J is the permeate flux [kg m^{-2} h^{-1}], Δm_p is the mass of collected permeate, A is the

effective membrane area, Δt is the elapsed time, WF is the wetting factor, J_i and J_t are the mean initial permeate flux and mean permeate flux at time t, CF is the concentration factor, M_{Fi} is the initial feed mass, M_{Pj} final obtained permeate mass at step j [kg] and WR is the water recovery, respectively. Step j corresponds to each sequential addition of surfactant to the feed. Every step took at least 30 minutes in which the experimental values were recorded every 10 minutes and their averages were considered during that step for each experimental setup. Salt concentrations of feed and permeate were correlated by feed and permeate electrical conductivity (supporting information).

4. Results and discussion

The wetting occurrence depends on several parameters such as intrinsic characteristics of the porous material, operating pressure conditions, and nature of the feed solutions [43]. When the membrane gets entirely wet it acts as a hydrophilic microfiltration membrane because of the large pore size, resulting in an increase in permeate flux and a dramatic decrease in salt rejection. As soon as the membrane is wetted, MD is not any more selective and thus does not fulfill its purpose of desalination or other kinds of separation. Pore wetting degrades the capabilities of the MD systems either because it lowers the interface for evaporation and hence the formation of vapor, or because when a pore is wetted saline liquid feed may run through and contaminate the permeate [44].

By the addition of surfactants into the membrane cell, they begin to enter the membrane interface, decreasing the membrane surface free energy by:

- reducing the energy of the interface [45], and
- covering hydrophobic groups at the membrane surface with hydrophilic surfactant molecules

By increasing the concentration of the surfactant in the system, micellization may happen (aggregation of surfactant molecules). The minimum concentration at which micellization starts is known as the critical micelle concentration (CMC) [46]. Prior to attaining the CMC, the surface tension varies intensely with the concentration of the surfactant. When the CMC is reached, the surface tension stays comparatively unchanging or alters with a lesser slope. The CMC strongly depends on pressure, temperature, and on the existence and concentration electrolytes and of other surface-active species. For instance, the aggregation number for SDS rises with increasing amounts of the electrolyte NaCl, while CMC decreases [47]. Fig. 3 illustrates the surface tension versus SDS concentrations at eleven fixed concentrations of NaCl [48].

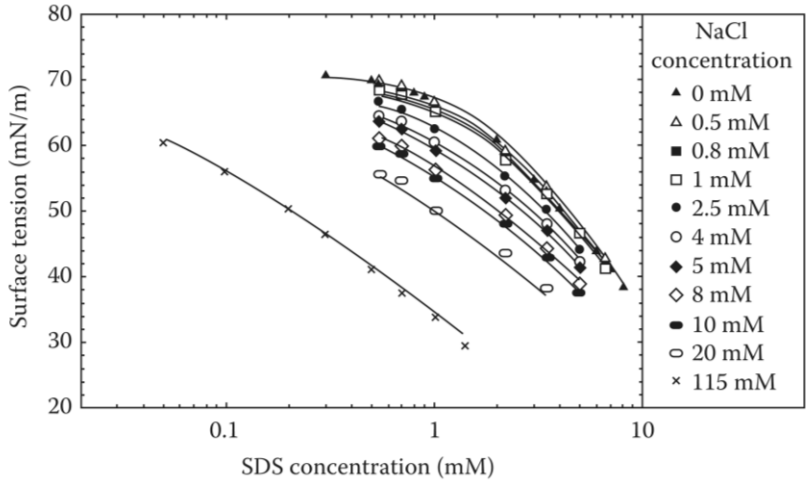

Fig. 3. Surface tension as a function of the concentration of SDS for eleven fixed NaCl concentrations[48]

SDS creates spherical micelles at low NaCl concentrations (<0.45 M), however, it forms rod-like micelles at high NaCl concentrations at which its micelle concentration is high [49]. Mostly, the micelle size reduces with the increase of temperature for SDS. The rod-like micelle produced at high NaCl concentrations reduces its size approximately five times more intensely than the spherical micelle by increasing the temperature [46].

4.1 Effect of high salinity feed on wetting

At the beginning of the experiments E1 to E4, when NaCl was added to the deionized water feed to make a 1.0 M solution, the permeate flux across the membrane negligibly decreased (Fig. 4a-d). These results are in principle in accordance with other reports [50] as the adding non-volatile solutes to water leads to concentration boundary layer adjacent to the feed membrane surface. This reduces the partial vapor pressure of the system and accordingly lowers the driving force of the system. Additionally, when salt was added to the feed in the setups E1 to E4, the permeate electrical conductivity was slightly increased.

Generally, the presence of salt in the distillate can be attributed either to entrainment of fine liquid droplets by vapor molecules [51] or to membrane pore wetting [52]. It these setups, high salt concentration did not cause complete pore wetting because the permeate flux did not increase. However, since the membrane pores are considerably larger (0.2 μm) than the ionic radius of Na^+ and Cl^-, the NaCl passage in the hydrophobic membranes happens primarily caused by the entrainment of fine liquid droplets in the vapor phase. The ionic radius of Na^+ and Cl^- are 1.02 and 1.81 Å, respectively [53]. The improvement in salt rejection for superhydrophobic membranes is attributed to the relatively higher vapor flux and the rejection of liquid phase caused by higher hydrophobicity (setup E5). This phenomenon has been reported before [26].

Ultimately, the combination of air recharging, mesh spacer and superhydrophobic membrane in setup E6 resulted in no increase in permeate electrical conductivity and permeate flux at the beginning of the experiment. This can be attributed to the reduction of the salt boundary layer near the feed membrane surface.

4.2 Effect of air recharging

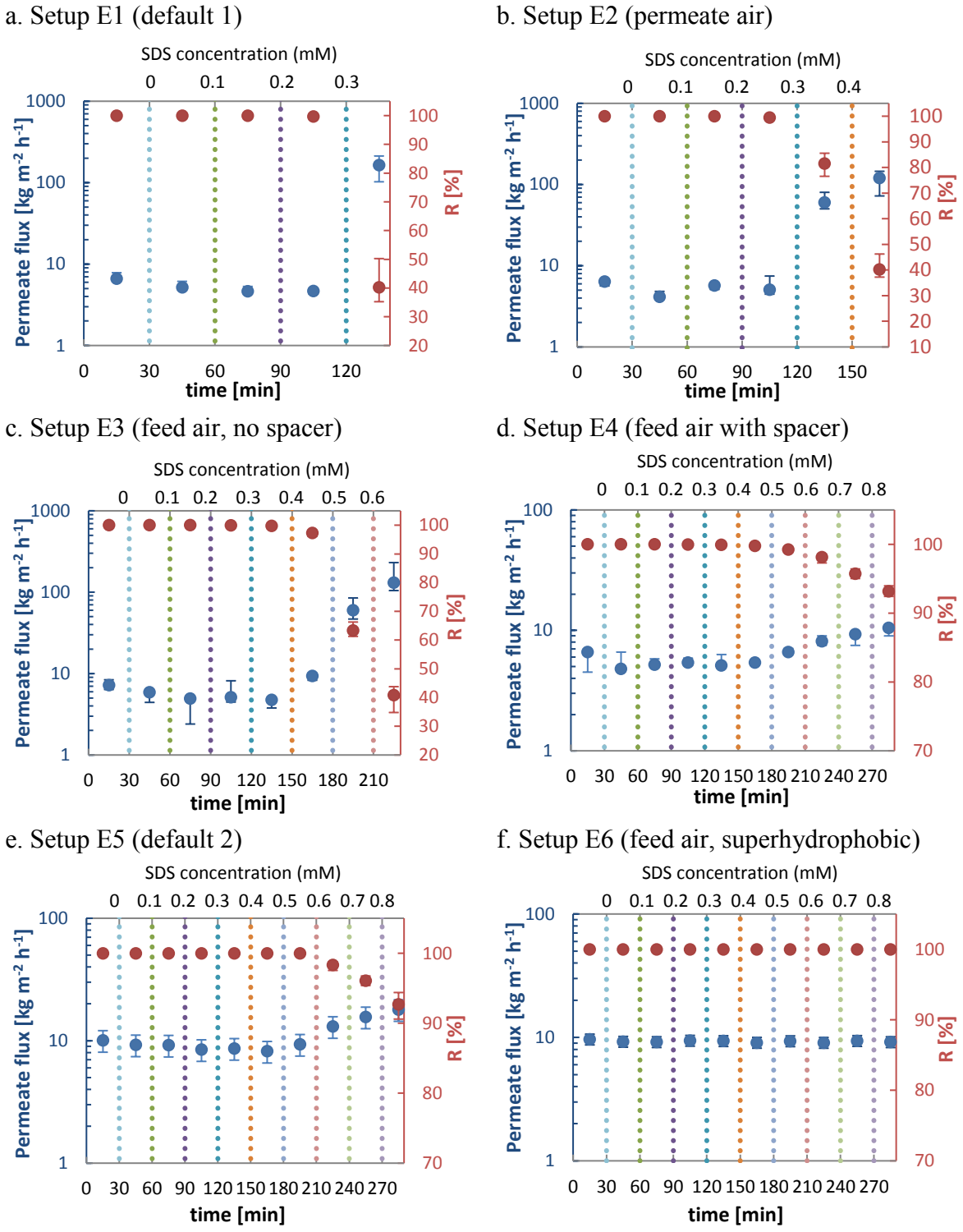

Fig. 4. The permeate flux (● J) and salt rejection (● R) for setups E1-E6. The mean temperature of feed and permeate were 60 °C and 20 °C, respectively. The round vertical dots show the SDS concentration in the feed. NaCl was added after 30 minutes to make the 1.0 M saline solution.

Fig. 4 shows the permeate fluxes and salt rejections overtime for the setups E1 to E6. The polypropylene membrane without air recharging and mesh spacer on the feed side was first used as a default case to measure the reference permeate flux and salt rejection in the setup E1. It is worth noting that the pressure caused by air bubbles in the membrane cell must be less than the critical pressure of liquid entering membrane pores. By adding SDS to the concentration of 0.3 mM the salt rejection dramatically decreased to 40% and permeate flux increased from 4.7 to 164.4 kg/m^2-h (Fig. 4a). The high conductivity of the permeate at 105 minutes indicated the membrane wetting from that time onwards and poor salt rejection. In this case, liquid-wicking led to a direct connection between both feed and permeate, and because of that produced a sharp loss of selectivity.

In the next setup (experiment E2), air bubbles were introduced on the permeate side of the membrane and the mesh spacers were placed on both side of the membrane. Air recharging in the permeate side did a little and delayed the membrane pore wetting to SDS concentration of 0.4 mM. This was due to increasing pressure on the permeate side of the membrane, decreasing the transmembrane pressure difference and therefore increasing LEP (Fig. 4b). When air recharging without a mesh spacer in the membrane feed side (experiment E3) was used in the setup, the membrane held up for up to 0.4 mM SDS concentration until the pore wetting happened. Then, by adding more SDS into the feed, feed contaminated the distillate, therefore, permeate quality was dramatically affected and the salt rejection dropped sharply to ~40% and permeate flux raised from 4.7 to 131.2 kg/m^2-h (Fig. 4c).

Surface wetting of hydrophobic membranes happens when hydrophilic groups (e.g., C=O, OH, and COOH) forms on the polypropylene surface [54]. But, when the air bubbles are introduced in the feed, SDS diffuses in water molecules and adsorb at the interfaces of air and water. The water-

indissoluble hydrophobic hydrocarbon tails may reach out of the bulk water phase, into the air, whereas the water-dissoluble head stays in the water phase. In this case, hydrophobic (or non-wetting) parts of surfactant dispersed in water easily attach to air bubbles, preventing the hydrophilic parts wet the membrane surface.

4.3 Effect of mesh spacer and air recharging

In the experiment E4, a mesh spacer was placed near the surface of the membrane on the feed side and air bubbles were introduced to the feed side of the membrane cell. The existence of the mesh spacer led to trapping air bubbles on the membrane surface and consequently reducing the cohesion of surfactant to the membrane surface. Although the mesh spacer remitted the occurrence of pore wetting compare to the experiment E3, for more SDS concentration in the feed the system experienced wetting and the salt rejection dropped to 92% (Fig. 4d). This pore wetting might be referred to this fact which the larger pores and the capillary force processed smaller hindrance for water penetration [55].

4.4 Effect of membrane superhydrophobicity

In the experiment E5, the superhydrophobic PTFE/PES membrane was used in the setup instead of the hydrophobic PP membrane. Without introducing air bubbles in the feed side over the first 3 h, the strong superhydrophobic properties of these membranes retarded the pores wetting and no pore wetting was observed. Nonetheless, by increasing the SDS concentration more than 0.6 mM, the hydrophobicity of the membrane was compromised and the permeate electrical conductivity rose to 8 mS/cm, proving the superhydrophobicity was not able to resist the wetting solely for high surface-active species in the feed solution (Fig. 4e). Therefore, the robustness of such membranes was not guaranteed as they are susceptible to wetting for the high surfactant concentration in feed.

It is worth to note that a study of the effect of the hydrophobicity demonstrated that higher hydrophobicity led to a reduction of partial pore wetting and therefore maintaining the vapor transport for the entire range of pore sizes of the membrane [56]. Modifications of surface energy have several consequences which result in enhanced permeability deviations and clarify the domination of the PTFE membranes over PP membranes.

4.5 Effect of membrane superhydrophobicity with mesh spacer and air recharging

When superhydrophobic membrane with air recharging and the mesh spacer (experiment 6) in the membrane feed cell were implemented the setup prevented the pore wetting incident for even up to 0.8 mM SDS concentration in the feed and the distillate product was salt-free and salt rejection remained >99.9% (Fig. 4f). Dispersing the air bubbles into the feed increases the saturation of the absorbed air in the liquid phase and as in the pore structures the pressure lowers, the dissolved air is desorbed at the entrance of pores and displaces the liquid which partly tends to penetrate the macroporous structure. In this case, the trapped air bubbles combined with superhydrophobicity of the membrane resulted in the formation of high static contact angle while simultaneously decreased the area of feed in contact with the membrane and reduced adhesion of the surface-active species to the membrane surface. As it is observed in Fig. 4f, trapped air bubbles had no undesirable effect on the permeate flux.

For the comparison of both the best and worst scenarios for wetting prevention (setup E6 and E1 respectively), Fig. 5 shows in detail the process conditions (i.e., mean permeate and feed temperatures, transmembrane pressure difference, and permeate flux). In Fig.5a for the setup E1, there are three zones. In the first zone, the effect of feed temperature on flux is depicted.

By increasing the feed temperature from 40°C to 60°C, the flux increased by almost three times. In zone two, the addition of NaCl in the feed caused a slight decrease in the permeate flux as the salt decreased the vapor pressure of the solution [57]. In the last zone, wetting started to happen, seen in the increasing permeate flux, increasing permeate temperature, and the dropping of the transmembrane pressure difference along with the feed temperature. In contrast, in Fig.5b, because of a wetting hindrance in setup E6, permeate flux, transmembrane pressure difference, and mean temperatures stayed constant.

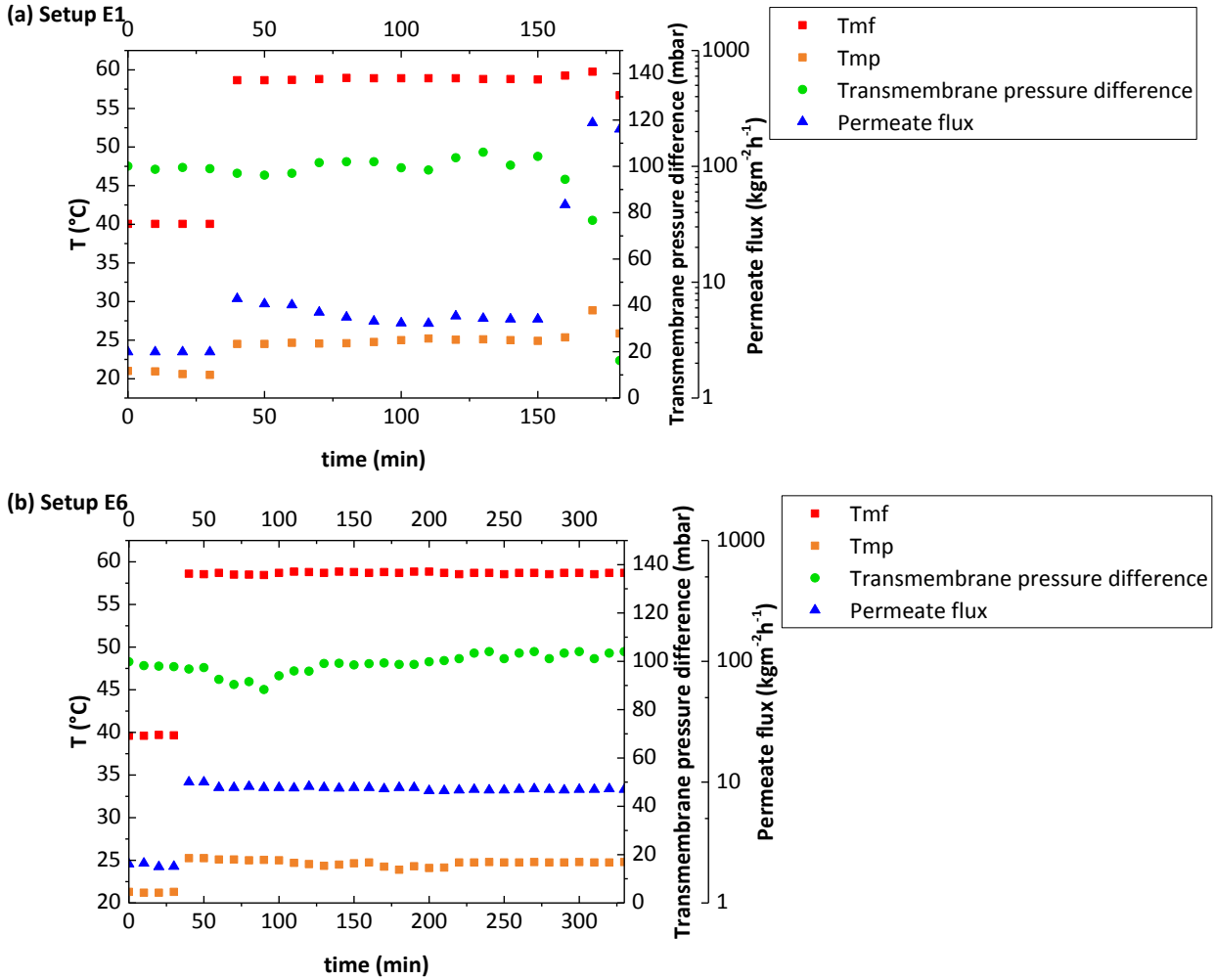

Fig. 5. Mean permeate and feed temperatures, transmembrane pressure difference and permeate flux for the setup E1 (a) and E6 (b). Zone 1, 2 and 3 refer to the elapsed times for the feed temperature elevation, non-wetted and wetted conditions, respectively.

Fig. 6 shows that recharging the air bubbles on the feed side of the membrane had no undesirable effect on the permeate flux, despite a potential diffusion resistance to water vapor introduced by the air layers. This can be explained by several factors. First, the air-covered areas still experience evaporation at the air-water interface similar to that at the air-water interface in MD membrane pores. Additionally, vapor transport may be improved by enhanced local agitation, reduced salt/surfactant deposition/adhesion on the membrane surface/pores, and reduced temperature and concentration polarization effects in the feed-membrane boundary layers [58].

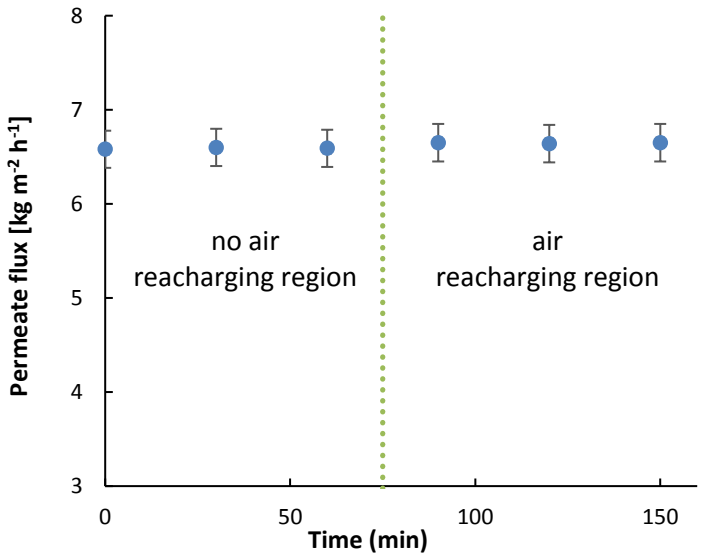

Fig. 6. Effect of air recharging introduction on the permeate flux

Fig. 7 shows the flow of the air bubbles on the membrane surface. One of the advantages of air bubble recharging was the creation of a condition in the system similar to froth flotation, in which the bubble foams were created by the air flow in the feed solution. These foams could be later collected in the feed tank which may be resulting in the reduction of the surfactant in the solution.

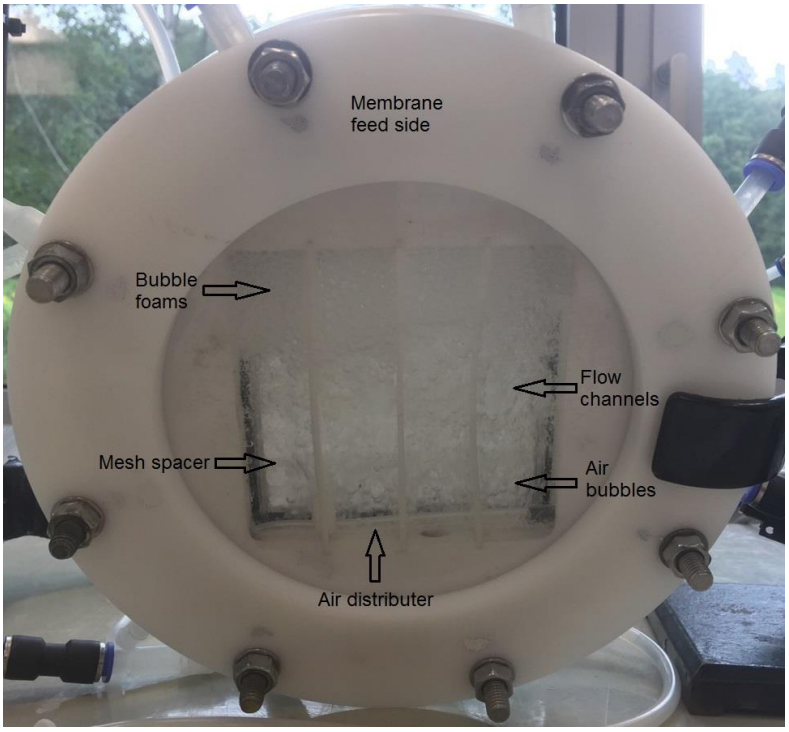

Fig. 7. Air recharging at the membrane surface for the setup E6 (wetting preventing setup). The air bubbles created bubble foams which can be collected in the feed.

Fig. **8** shows the wetting factor for the experiments E1 to E6. The wetting factor is defined as the relative permeate flux at the end of the experiment to the initial permeate flux without wetting. It is clear from Fig. 8 that E1 setup had the most wetting and E6 setup experienced no wetting.

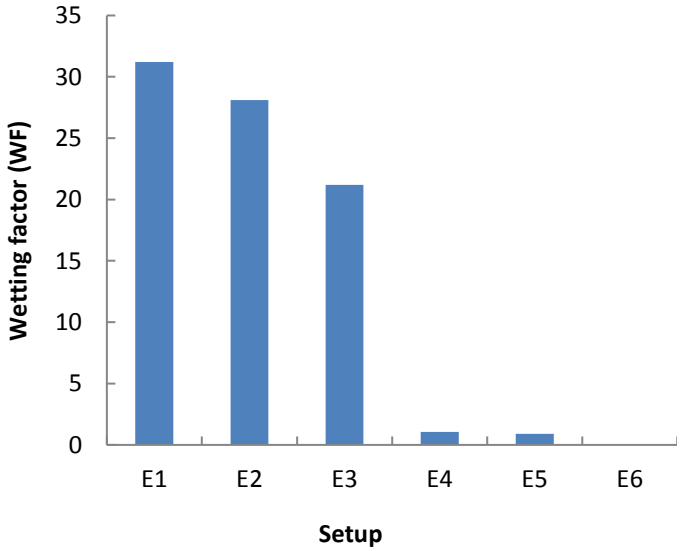

Fig. 8. Wetting factor for the setups E1-E6.

Moreover, Fig. 9 depicts the relationship between wetting rate and permeate flux for the E1-E5 setups. The wetting rate is calculated as the slope of the recorded rise in conductivity in µS cm^{-1} min^{-1}. In general, the higher the flux after wetting, the lower the salt rejection, wetting time, and the wetting rate. Using air bubbles together with mesh spacer in the feed side and the superhydrophobic membrane led to the suppression of wetting as the wetting rate decreased while the permeate flux did not rise.

Finally, the concentration factor and water recovery were considerably affected by wetting (Fig. 10). For the experiments E1 to E3, the wetting magnitude was high, and therefore the high amount of liquid feed was passed through the membrane and affected the water recovery and concentration factor, while in setups E4 to E6 because of less wetting amounts the concentration factor and water recovery did not rise significantly.

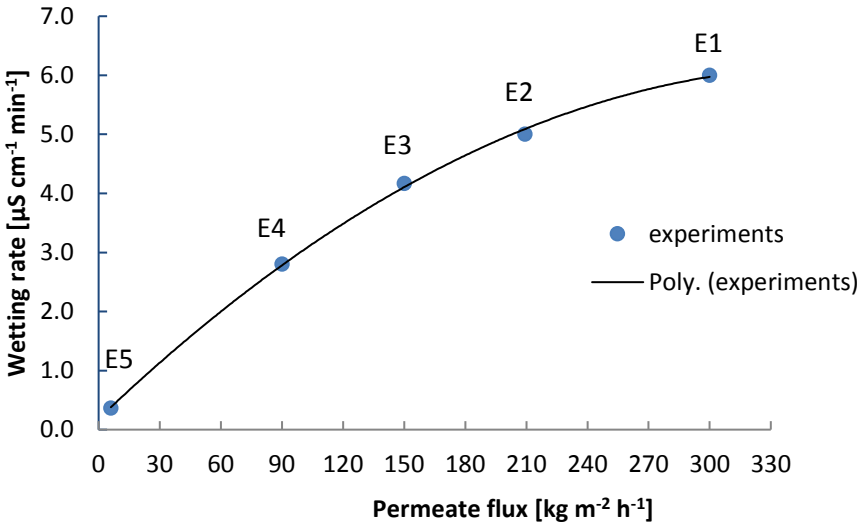

Fig. 9. Wetting rate and permeate flux after wetting has occurred.

Moreover, as it can be seen in Fig. 10, although during the course of the desalination in the setups E4-E6 the feed solutions were concentrated up to 40% from the initial concentration of 1.0 M, the system hindered the wetting incident. Higher salinities of feed solution will further reduce

surface tension and LEP (according to the Young-Laplace Equation) and has been studied in other work by the authors [59,60].

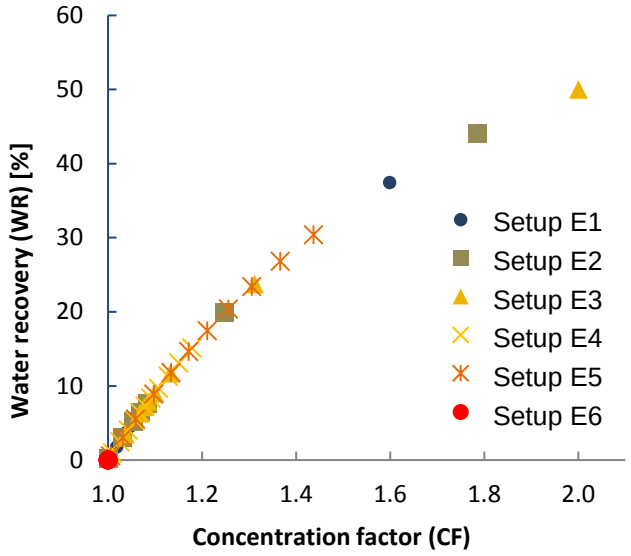

Fig. 10. Water recovery versus concentration factor.

5. Conclusions

This study performed the first application of a new wetting prevention technique in a full MD setup: maintaining active air layers on an MD membrane surface. To develop this new approach, this study varied the membrane type, membrane hydrophobicity, application site of air, and the concentration of a surfactant which was used to cause wetting. Wetting in the MD process was best prevented by applying air bubbles on the membrane surface on the feed side in combination with superhydrophobic membranes, which was extremely effective and fully prevented wetting. This finding is consistent with the theory of Chandler [61] which shows that trapped air bubbles result in the formation of discontinuous three phase contact line and high static contact angle. Moreover, air recharging reduced the contact area of the membrane with the feed solution and consequently reduced the adhesion of surfactant to the membrane surface.

The most promising result for wetting prevention was achieved through using a PTFE superhydrophobic membrane in conjunction with airflow and a mesh spacer on the feed side. Even after reaching of 0.8 mM SDS concentration in the solution, no wetting occurred. Meanwhile, the default setup with a polypropylene hydrophobic membrane without the introduction of airflow or mesh spacer was the most vulnerable setup to the wetting incident, with wetting quickly occurring at concentrations as low as 0.3 mM SDS. In this setup, pore wetting led to penetration of liquid water and affected the quality of fresh water produced.

A surprising observation in this study of the wetting phenomenon in MD was that the presence of a mesh spacer on the feed side of the membrane cell was vital for preventing wetting. This can be explained by the importance of the spacer trapping and maintaining the air bubbles on the membrane surface to avoid the direct bond of the hydrophilic tail of the surface-active species with the polymeric membrane surface.

Appendix A

Fig. A.1 shows the electrical conductivity versus salt concentration which is used for calculating salt rejection. These measurements were made in triplicate and represent a relative standard deviation of less than 3%.

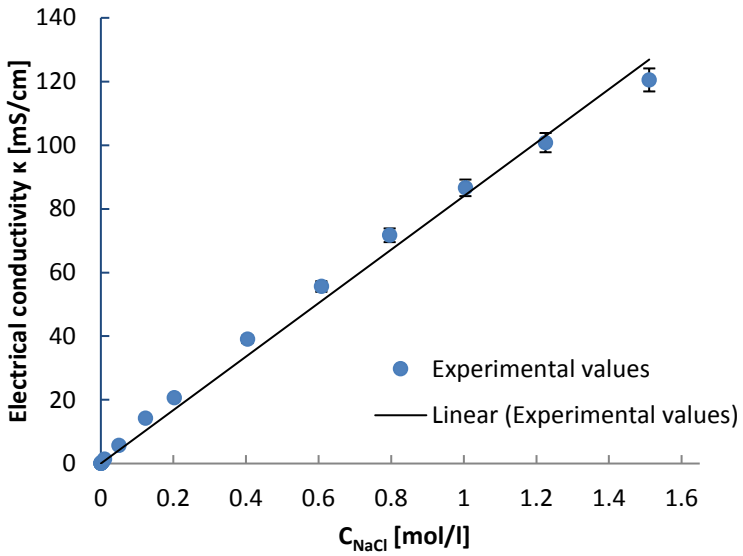

Fig. A.1: Electrical conductivity and NaCl concentration calibration line ($\kappa=83.99C_{NaCl}$, $R^2=0.9943$).

Funding

This research did not receive any specific grant from funding agencies in the public, commercial, or not-for-profit sectors.

Author Contributions

Mohammad Rezaei performed and analyzed the experiments, wrote almost all sections and created all figures excluding those credited to other authors below. David M. Warsinger helped in designing and planning the experiments, wrote section 2, partially section 1 and created figure 1, with its associated calculations. Warsinger carried out the first level editing. John Lienhard

performed vital corrections on the manuscript. Wolfgang M. Samhaber supervised, provided guidance and edited the abstract. All authors assisted with reviewing and revising the manuscript. All authors have given approval to the final version of the manuscript.

Notes

The authors declare no competing financial interest.

Nomenclature

$C_{b,p}$, concentration in permeate solution [mol/l]; $C_{b,f}$, concentration in bulk feed solution [mol/l]; CF, concentration factor [-]; f_1, area fractions of material 1; f_2, area fractions of material 2; J, permeate flux [kg/m²s]; LEP, liquid entry pressure [kPa]; M_{Fi}, initial feed mass [kg]; M_{Pj}, final obtained permeate mass at the end of stage j [kg]; R, salt rejection [%]; t, operating time [h]; Tm, mean temperature of $T_{m,f}$ & $T_{m,p}$ [°C]; $T_{m,f}$, feed temperature at the membrane [°C]; $T_{m,p}$, permeate temperature at the membrane [°C]; WF, wetting factor [-]; WR, water recovery [%]; θ_1, contact angles for the material 1; θ_2, contact angles for the material 2; θ_c, effective contact angle.

References

[1] D. Warsinger, J. Swaminathan, J.H. Lienhard, Effect of Module Inclination Angle on Air Gap Membrane Distillation, in: Proc. 15th Int. Heat Transf. Conf., Begellhouse, Connecticut, 2014: pp. 1–14. doi:10.1615/IHTC15.mtr.009351.

[2] D.E.M. Warsinger, J. Swaminathan, C.H. Won, S. Jeong, J.H.L. V, The Effect of Filtration and Particulate Fouling in Membrane Distillation, Int. Desalin. Assoc. World Congr. Desalin. Water Reuse. (2015). https://dspace.mit.edu/handle/1721.1/100445 (accessed July 25, 2016).

[3] Z. Ma, Y. Hong, L. Ma, M. Su, Superhydrophobic Membranes with Ordered Arrays of Nanospiked Microchannels for Water Desalination, Langmuir. 25 (2009) 5446–5450. doi:10.1021/la900494u.

[4] D.M. Warsinger, J. V Gonzalez, S.M. Van Belleghem, A. Servi, J. Swaminathan, J.H.L. V, The Combined Effect of Air Layers and Membrane Superhydrophobicity on Biofouling in Membrane Distillation, Am. Water Work. Assoc. Annu. Conf. Expo. (2015).

[5] D.M. Warsinger, A. Servi, S. Van Belleghem, J. Gonzalez, J. Swaminathan, J. Kharraz, H.W. Chung, H.A. Arafat, K.K. Gleason, J.H. Lienhard V, Combining air recharging and membrane superhydrophobicity for fouling prevention in membrane distillation, J. Memb. Sci. 505 (2016) 241–252. doi:10.1016/j.memsci.2016.01.018.

[6] M.R. Qtaishat, F. Banat, Desalination by solar powered membrane distillation systems, Desalination. 308 (2013) 186–197. doi:10.1016/j.desal.2012.01.021.

[7] K.W. Lawson, D.R. Lloyd, Membrane distillation, J. Memb. Sci. 124 (1997) 1–25. doi:10.1016/S0376-7388(96)00236-0.

[8] N.M. Mokhtar, W.J. Lau, B.C. Ng, A.F. Ismail, D. Veerasamy, Preparation and characterization of PVDF membranes incorporated with different additives for dyeing solution treatment using membrane distillation, Desalin. Water Treat. 56 (2015) 1999–2012. doi:10.1080/19443994.2014.959063.

[9] K. Smolders, A.C.M. Franken, Terminology for Membrane Distillation, Desalination. 72 (1989) 249–262. doi:10.1016/0011-9164(89)80010-4.

[10] K.Y. Wang, S.W. Foo, T.-S. Chung, Mixed Matrix PVDF Hollow Fiber Membranes with

Nanoscale Pores for Desalination through Direct Contact Membrane Distillation, Ind. Eng. Chem. Res. 48 (2009) 4474–4483. doi:10.1021/ie8009704.

[11] M.R. Bilad, E. Guillen-Burrieza, M.O. Mavukkandy, F.A. Al Marzooqi, H.A. Arafat, Shrinkage, defect and membrane distillation performance of composite PVDF membranes, Desalination. 376 (2015) 62–72. doi:10.1016/j.desal.2015.08.015.

[12] Y. Shin, H. Cho, J. Choi, Y. Sun Jang, Y.-J. Choi, J. Sohn, S. Lee, J. Choi, Application of response surface methodology (RSM) in the optimization of dewetting conditions for flat sheet membrane distillation (MD) membranes, Desalin. Water Treat. 57 (2016) 10020–10030. doi:10.1080/19443994.2015.1038114.

[13] A.M. Alklaibi, N. Lior, Membrane-distillation desalination: Status and potential, Desalination. 171 (2005) 111–131. doi:10.1016/j.desal.2004.03.024.

[14] P.-J. Lin, M.-C. Yang, Y.-L. Li, J.-H. Chen, Prevention of surfactant wetting with agarose hydrogel layer for direct contact membrane distillation used in dyeing wastewater treatment, J. Memb. Sci. 475 (2015) 511–520. doi:10.1016/j.memsci.2014.11.001.

[15] Z. Wang, J. Jin, D. Hou, S. Lin, Tailoring surface charge and wetting property for robust oil-fouling mitigation in membrane distillation, J. Memb. Sci. 516 (2016) 113–122. doi:10.1016/j.memsci.2016.06.011.

[16] E. Guillen-Burrieza, A. Servi, B.S. Lalia, H.A. Arafat, Membrane structure and surface morphology impact on the wetting of MD membranes, J. Memb. Sci. 483 (2015) 94–103. doi:10.1016/j.memsci.2015.02.024.

[17] R.B. Saffarini, B. Mansoor, R. Thomas, H.A. Arafat, Effect of temperature-dependent

microstructure evolution on pore wetting in PTFE membranes under membrane distillation conditions, J. Memb. Sci. 429 (2013) 282–294. doi:10.1016/j.memsci.2012.11.049.

[18] J.A. Prince, D. Rana, T. Matsuura, N. Ayyanar, T.S. Shanmugasundaram, G. Singh, Nanofiber based triple layer hydro-philic/-phobic membrane - a solution for pore wetting in membrane distillation, Sci. Rep. 4 (2014) 6949. doi:10.1038/srep06949.

[19] D.-H. Jung, I.J. Park, Y.K. Choi, S.-B. Lee, H.S. Park, J. Rühe, Perfluorinated Polymer Monolayers on Porous Silica for Materials with Super Liquid Repellent Properties, Langmuir. 18 (2002) 6133–6139. doi:10.1021/la025558u.

[20] H. Liu, W. Yang, Y. Ma, Y. Cao, J. Yao, J. Zhang, T. Hu, Synthesis and Characterization of Titania Prepared by Using a Photoassisted Sol−Gel Method, Langmuir. 19 (2003) 3001–3005. doi:10.1021/la026600o.

[21] A. Razmjou, E. Arifin, G. Dong, J. Mansouri, V. Chen, Superhydrophobic modification of TiO2 nanocomposite PVDF membranes for applications in membrane distillation, J. Memb. Sci. 415–416 (2012) 850–863. doi:10.1016/j.memsci.2012.06.004.

[22] S. Lin, S. Nejati, C. Boo, Y. Hu, C.O. Osuji, M. Elimelech, Omniphobic Membrane for Robust Membrane Distillation, Environ. Sci. Technol. Lett. 1 (2014) 443–447. doi:10.1021/ez500267p.

[23] F. Guo, A. Servi, A. Liu, K.K. Gleason, G.C. Rutledge, Desalination by Membrane Distillation using Electrospun Polyamide Fiber Membranes with Surface Fluorination by Chemical Vapor Deposition, ACS Appl. Mater. Interfaces. 7 (2015) 8225–8232. doi:10.1021/acsami.5b01197.

[24] X. Li, X. Yu, C. Cheng, L. Deng, M. Wang, X. Wang, Electrospun Superhydrophobic Organic/Inorganic Composite Nanofibrous Membranes for Membrane Distillation, ACS Appl. Mater. Interfaces. 7 (2015) 21919–21930. doi:10.1021/acsami.5b06509.

[25] Z.-Q. Dong, B.-J. Wang, X. Ma, Y.-M. Wei, Z.-L. Xu, FAS Grafted Electrospun Poly(vinyl alcohol) Nanofiber Membranes with Robust Superhydrophobicity for Membrane Distillation, ACS Appl. Mater. Interfaces. 7 (2015) 22652–22659. doi:10.1021/acsami.5b07454.

[26] K. Gethard, O. Sae-Khow, S. Mitra, Water Desalination Using Carbon-Nanotube-Enhanced Membrane Distillation, ACS Appl. Mater. Interfaces. 3 (2011) 110–114. doi:10.1021/am100981s.

[27] X. Li, C. Wang, Y. Yang, X. Wang, M. Zhu, B.S. Hsiao, Dual-Biomimetic Superhydrophobic Electrospun Polystyrene Nanofibrous Membranes for Membrane Distillation, ACS Appl. Mater. Interfaces. 6 (2014) 2423–2430. doi:10.1021/am4048128.

[28] E. Guillen-Burrieza, M.O. Mavukkandy, M.R. Bilad, H.A. Arafat, Understanding wetting phenomena in membrane distillation and how operational parameters can affect it, J. Memb. Sci. 515 (2016) 163–174. doi:10.1016/j.memsci.2016.05.051.

[29] S. Goh, J. Zhang, Y. Liu, A.G. Fane, Fouling and wetting in membrane distillation (MD) and MD-bioreactor (MDBR) for wastewater reclamation, Desalination. 323 (2013) 39–47. doi:10.1016/j.desal.2012.12.001.

[30] L. Martínez-Díez, M.I. Vázquez-González, F.J. Florido-Díaz, Study of membrane distillation using channel spacers, J. Memb. Sci. 144 (1998) 45–56. doi:10.1016/S0376-

7388(98)00024-6.

[31] J. Phattaranawik, R. Jiraratananon, A.. Fane, C. Halim, Mass flux enhancement using spacer filled channels in direct contact membrane distillation, J. Memb. Sci. 187 (2001) 193–201. doi:10.1016/S0376-7388(01)00344-1.

[32] Y.M. Manawi, M. Khraisheh, A.K. Fard, F. Benyahia, S. Adham, Effect of operational parameters on distillate flux in direct contact membrane distillation (DCMD): Comparison between experimental and model predicted performance, Desalination. 336 (2014) 110–120. doi:10.1016/j.desal.2014.01.003.

[33] G. Chen, X. Yang, R. Wang, A.G. Fane, Performance enhancement and scaling control with gas bubbling in direct contact membrane distillation, Desalination. 308 (2013) 47–55. doi:10.1016/j.desal.2012.07.018.

[34] D.E.M.M. Warsinger, J. Swaminathan, L.A. Maswadeh, J.H. Lienhard V, J.H. Lienhard, Superhydrophobic condenser surfaces for air gap membrane distillation, J. Memb. Sci. 492 (2015) 578–587. doi:10.1016/j.memsci.2015.05.067.

[35] A. Katsandri, A theoretical analysis of a spacer filled flat plate membrane distillation modules using CFD: Part I: velocity and shear stress analysis, Desalination. (2015) 1–21. doi:10.1016/j.desal.2015.09.001.

[36] G.J. Hirasaki, Wettability: Fundamentals and Surface Forces, SPE Form. Eval. 6 (1991) 217–226. doi:10.2118/17367-PA.

[37] L. Eykens, K. De Sitter, C. Dotremont, L. Pinoy, B. Van der Bruggen, Characterization and performance evaluation of commercially available hydrophobic membranes for direct

contact membrane distillation, Desalination. 392 (2016) 63–73. doi:10.1016/j.desal.2016.04.006.

[38] M. Shakaib, S.M.F. Hasani, I. Ahmed, R.M. Yunus, A CFD study on the effect of spacer orientation on temperature polarization in membrane distillation modules, Desalination. 284 (2012) 332–340. doi:10.1016/j.desal.2011.09.020.

[39] M.M.A. Shirazi, A. Kargari, A.F. Ismail, T. Matsuura, Computational Fluid Dynamic (CFD) opportunities applied to the membrane distillation process: State-of-the-art and perspectives, Desalination. 377 (2016) 73–90. doi:10.1016/j.desal.2015.09.010.

[40] M. Rezaei, W.M. Samhaber, Wetting Behaviour of Superhydrophobic Membranes Coated with Nanoparticles in Membrane Distillation, Chem. Eng. Trans. 47 (2016) 373–378. doi:10.3303/CET1647063.

[41] M. Khayet, M.P. Godino, J.I. Mengual, Theoretical and experimental studies on desalination using the sweeping gas membrane distillation method, Desalination. 157 (2003) 297–305. doi:10.1016/S0011-9164(03)00409-0.

[42] H. Groothuis, W.P. Hendal, Heat transfer in Two-Phase flow, Chem. Eng. Sci. 11 (1959) 212–220.

[43] M. Courel, E. Tronel-Peyroz, G.M. Rios, M. Dornier, M. Reynes, The problem of membrane characterization for the process of osmotic distillation, Desalination. 140 (2001) 15–25. doi:10.1016/S0011-9164(01)00351-4.

[44] D.M. Warsinger, J. Swaminathan, E. Guillen-Burrieza, H.A. Arafat, J.H. Lienhard V, Scaling and fouling in membrane distillation for desalination applications: A review,

Desalination. 356 (2015) 294–313. doi:10.1016/j.desal.2014.06.031.

[45] F. Hakiki, D.A. Maharsi, T. Marhaendrajana, Surfactant-Polymer Coreflood Simulation and Uncertainty Analysis Derived from Laboratory Study, J. Eng. Technol. Sci. 47 (2015) 706–725. doi:10.5614/j.eng.technol.sci.2015.47.6.9.

[46] P.C. Hiemenz, R. Rajagopalan, Principles of Colloid and Surface Chemistry, Third edit, Marcel Dekker, Inc., 1997.

[47] G. Dupla, S. Cedex, M.F.F. Marques, Size of Sodium Dodecyl Sulfate Micelles in Aqueous Solutions as Studied by Positron Annihilation Lifetime Spectroscopy, J. Phys. Chem. 3654 (1996) 16608–16612.

[48] K.S. Birdi, Handbook of Surface and Colloid Chemistry, Fourth edi, 2016.

[49] S. Hayashi, S. Ikeda, Micelle size and shape of sodium dodecyl sulfate in concentrated sodium chloride solutions, J. Phys. Chem. 84 (1980) 744–751. doi:10.1021/j100444a011.

[50] K. Schneider, W. Hölz, R. Wollbeck, S. Ripperger, Membranes and modules for transmembrane distillation, J. Memb. Sci. 39 (1988) 25–42. doi:10.1016/S0376-7388(00)80992-8.

[51] A. Criscuoli, M.C. Carnevale, Desalination by vacuum membrane distillation: The role of cleaning on the permeate conductivity, Desalination. 365 (2015) 213–219. doi:10.1016/j.desal.2015.03.003.

[52] J. Ge, Y. Peng, Z. Li, P. Chen, S. Wang, Membrane fouling and wetting in a DCMD process for RO brine concentration, Desalination. 344 (2014) 97–107. doi:10.1016/j.desal.2014.03.017.

[53] J. Burgess, Ions in Solution: Basic Principles of Chemical Interactions, 1999.

[54] M. Gryta, Water desalination using membrane distillation with acidic stabilization of scaling layer thickness, Desalination. 365 (2015) 160–166. doi:10.1016/j.desal.2015.02.031.

[55] K. Chen, C. Xiao, Q. Huang, H. Liu, H. Liu, Y. Wu, Z. Liu, Study on vacuum membrane distillation (VMD) using FEP hollow fiber membrane, Desalination. 375 (2015) 24–32. doi:10.1016/j.desal.2015.07.021.

[56] L.F. Dumée, S. Gray, M. Duke, K. Sears, J. Schütz, N. Finn, The role of membrane surface energy on direct contact membrane distillation performance, Desalination. 323 (2013) 22–30. doi:10.1016/j.desal.2012.07.012.

[57] R.W. Baker, Membrane Technology and Applications, Second edi, John Wiley & Sons, Ltd, Chichester, UK, 2004. doi:10.1002/9781118359686.

[58] C. Wu, Z. Li, J. Zhang, Y. Jia, Q. Gao, X. Lu, Study on the heat and mass transfer in air-bubbling enhanced vacuum membrane distillation, Desalination. 373 (2015) 16–26. doi:10.1016/j.desal.2015.07.001.

[59] K. Govind, J. Swaminathan, D.M. Warsinger, G.H. Mckinley, J.H. Lienhard, Effect of scale deposition on surface tension of seawater and membrane distillation, Proc. Int. Desalin. Assoc. World Congr. Desalin. Water Reuse, San Diego, CA, USA. (2016).

[60] K.G. Nayar, D. Panchanathan, G.H. McKinley, J.H. Lienhard, Surface Tension of Seawater, J. Phys. Chem. Ref. Data. 43 (2014). doi:10.1063/1.4899037.

[61] K. Lum, D. Chandler, J.D. Weeks, Hydrophobicity at Small and Large Length Scales, J.

Phys. Chem. B. 103 (1999) 4570–4577. doi:10.1021/jp984327m.

Highlights

- For the first time, air recharging for wetting prevention in a full MD setup was examined.
- Air recharging combined with superhydrophobic membranes prevented wetting for low surface tension saline solutions with ~100% salt rejection.
- Our results suggest that air recharging is critical for MD applications with feed waters containing organic compounds or surfactants.

Graphical Abstract